A Coaxial Waveguide Commutator Feed for a Scanning Circular Phased Array Antenna

E. P. IRZINSKI

Abstract—**A coaxial waveguide amplitude commutation feed system has been developed for application to the scanning circular array antenna problem. A dominant TEM mode and a pair of orthogonal TE_{11} modes suitably excited at the input of a coaxial waveguide feed are employed to generate a simply commutatable low-sidelobe discrete amplitude distribution at the peripheral output ports of the coaxial circular array feed. The major advantages of the coaxial commutator feed compared to other circular array feed types are the broad bandwidth and small insertion loss simultaneously achieved with a simple feed geometry. The design and measured performance capability of a 30-percent RF bandwidth low-sidelobe coaxial commutator feed are described in detail.**

Introduction

The RF feed network design has long been recognized as the critical problem area in scanning circular array antenna systems. A fundamental requirement of the feed system is the capability to commutate a desirable amplitude distribution, usually tapered for low-sidelobe performance, about the periphery of the circular array in such a manner that a given number of radiating elements in a 180° or smaller sector is excited at any instant of time. The RF feed design tradeoff is usually one of physical complexity with the accompanying insertion-loss and tolerance control problems versus the ultimate desire of complete commutation capability of the ideal complex amplitude distribution, i.e., the desirable amplitude distribution magnitude and the requisite phase characteristics for plane-wave generation from a circular sector boundary. The network implementation problem is one of practical rather than theoretical realizability and a number of unique feed system designs have been developed to cope with the circular array geometry. Among these have been the R-2R lens feed [1], the Butler Matrix feed [2], the transfer switch matrix feed [3], and the waveguide commutator feed [4]. Various other feasible circular array feed designs have also appeared in the literature but these designs can essentially be categorized as one or a union of a number of these basic four feed types.

The referenced unique feed designs all possess the desired capability of performing the amplitude commutation function but each design is usually associated with one or more undesirable physical or performance attributes which most frequently reside in the areas of design complexity, RF output amplitude and phase tolerance control, insertion loss, or bandwidth limitations. The circular array feed network design reported upon in this short paper is characterized by design simplicity with a resultant significant overall improvement in the critical cited performance areas. The key element of this circular array feed design is a coaxial waveguide amplitude commutator similar in performance capability to the radial waveguide design developed previously [4] but without the bandwidth limitations inherent in this nonuniform transmission-line device [5]. The unique features of the coaxial waveguide amplitude commutation network are an extremely simple coaxial input prove excitation network and the capability of large RF bandwidth operation. A dominant TEM mode and a pair of orthogonal TE_{11} modes excited within the coaxial waveguide are employed to generate a commutatable low-sidelobe amplitude distribution about the circular periphery of the RF feed output. Experimental data are presented in this paper on a 30-percent bandwidth design.

Manuscript received September 23, 1980; revised October 28, 1980.

The author is with The Johns Hopkins University, Applied Physics Laboratory, Laurel, MD 20810.

Principle of Operation

A schematic of the coaxial waveguide commutation network is shown in Fig. 1. The RF input is divided into two outputs via the K_{db} coupler. One of these outputs is the input to the sum port of the monopulse comparator. The four outputs of the monopulse comparator are connected to four symmetrically disposed input probes of the coaxial waveguide commutator. Thus the sum input to the monopulse comparator excites the TEM mode in the coaxial waveguide. The second output from the K_{db} coupler is the input to the variable power divider network as shown. The variable RF power divider design is current state of art [6] and employs a magic tee, a 90° hybrid, and a pair of differential phase shifters which control the relative magnitudes of the RF outputs. A special and desirable feature of this variable power divider design is that the output ports phase track each other. These power divider outputs are the inputs to the difference ports of the monopulse comparator. Consequently, the variable power divider excites a pair of spatially orthogonal TE_{11} modes in the coaxial waveguide. The coaxial waveguide commutator is a traveling-wave device which is terminated in N arbitrary output ports symmetrically disposed with respect to the four input ports. In the coaxial waveguide annular output region, a radial electric field intensity of the form

$$V(\phi)=\left(\frac{1+A}{2}\right)+\left(\frac{1-A}{2}\right)\sin\alpha\sin\phi+\left(\frac{1-A}{2}\right)\cos\alpha\cos\phi \tag{1}$$

will exist by a superposition of the functionally orthogonal TEM and TE_{11} mode pairs. The first term on the right of (1) is the constant contribution from the TEM mode. The remaining two terms are characterized by the $\sin\phi$, $\cos\phi$, angular variation of the spatially orthogonal TE_{11} modes with the magnitude proportionality factors $\sin\alpha$, $\cos\alpha$ arising from the differential phase shift settings $(\alpha;(\pi/2)-\alpha)$ of the variable power divider. Equation (1) can be rewritten in the more recognizable cosine-squared-on-a-pedestal form as

$$V(\phi)=A+(1-A)\cos^2\tfrac{1}{2}(\phi-\alpha) \tag{2}$$

where the pedestal magnitude A is related to the coupling coefficient as

$$K_{db}=10\log\left(1+2\left(\frac{1+A}{1-A}\right)^2\right). \tag{3}$$

An inspection of (2) reveals that a tapered amplitude distribution proportional to $V(\phi)$ may be continuously commutated about the output periphery of the coaxial waveguide amplitude commutator by a continuous variation of α. Since the function of this device is to feed a circular array, however, a variation of α in discrete equal increments will provide the desirable coarse commutation capability required for this type of feed system. Thus the RF outputs of the coaxial commutator interface with an RF switch and phase-shifter network as shown in Fig. 1 prior to final termination at the radiating element inputs of the circular array. The RF phase shifters are employed for the dual functions of plane-wave collimation of the cylindrical wavefront and a fine beam steering capability between the coarse discrete beam positions provided by the amplitude commutation and switching

0018-9480/81/0300-0266$00.75

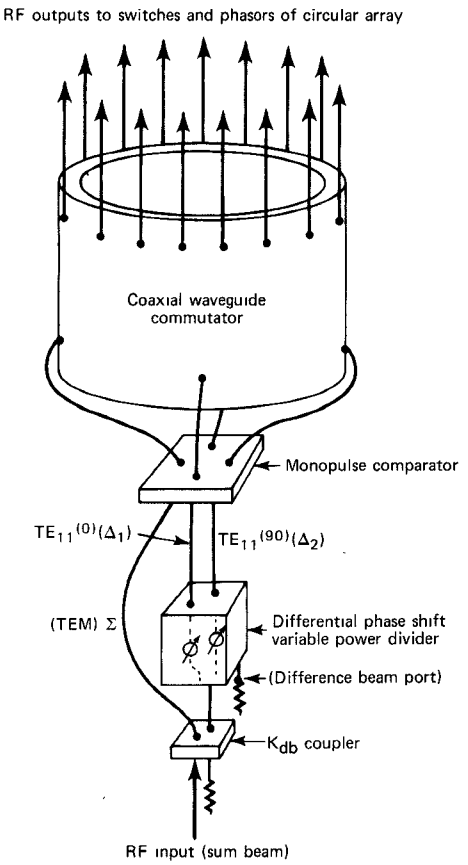

Fig. 1. Coaxial waveguide amplitude commutation network.

network. It may also be noted in Fig. 1 that a monopulse tracking capability may be added to the feed system by employing the isolated difference port of the variable power divider input.

Coaxial Waveguide Commutator Design

An experimental *L*-band model of a coaxial waveguide amplitude commutator was designed, fabricated, and tested to verify the feasibility of this circular array feed technique. A sketch of the waveguide commutator design is shown in Fig. 2. A design employing 16 output ports was chosen somewhat arbitrarily, however, this commutator would be compatible with a 64-element circular array employing 16-1P4T RF switches and 16 phase shifters for the excitation of a sector of 16 radiating elements at a given instant of time. The commutator dimensions were sized with manufacturing ease rather than physical compactness as guidelines. A uniform circular tube outer conductor and a linearly tapered coaxial inner conductor were employed to achieve a smooth TEM-dominant mode characteristic impedance transition from 12.5 Ω at the input probe plane to 3.125 Ω at the output probe plane. An outer conductor inside diameter of 7.5 in was chosen primarily to allow sufficient clearance for installation and modification of the input and output probe assemblies. The separation between the input and output probe planes was about 10 in. The commutator was designed with constant coaxial characteristic impedance section extensions of several inches on both ends of the commutator to allow for an independent probe-impedance tuning capability by adjustment of the individual sliding short mechanisms.

As is well known, the cutoff frequency of the TE_{11} mode as well as the higher order unwanted TE_{m1} modes decreases significantly in low TEM mode impedance coaxial waveguide [5]. The

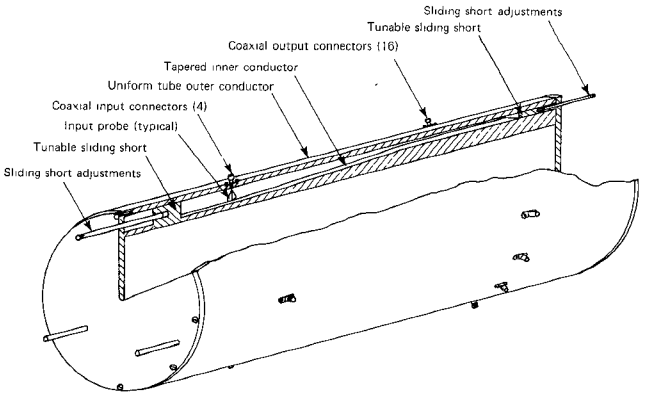

Fig. 2. Coaxial waveguide commutator geometry.

customary design procedure in such a situation would ordinarily be to size the coaxial waveguide to prohibit the propagation of the first or lowest cutoff frequency undesirable higher order mode in the frequency band of interest. A smaller diameter design would, however, place an undesirable burden on the mechanical design in the probe implementation and circumferential spacing as well as the tolerance control areas. The chosen outer diameter of 7.5 in allows propagation of the TE_{21} mode in approximately the upper 2/3 of the 30-percent frequency band for which the experimental data reported in this short paper were measured. The excitation of the TE_{21} mode, or a spurious or nonorthogonal TE_{11} mode for that matter, is most likely to result from unbalanced input probe voltages that occur because of external effects, such as monopulse comparator output imbalance, or from input probe mechanical irregularities. The results of the test program have confirmed that higher order TE_{21} mode excitation is not a major problem area in this type of circular array feed design provided that the input probe excitation levels are reasonably well balanced.

Experimental Program

An extensive developmental test program was conducted on the coaxial waveguide amplitude commutator in essentially two stages. The initial stage was devoted to the commutator input and output probe impedance matching for the TEM and the pair of orthogonal TE_{11} modes. The VSWR measurements were made at the appropriate inputs of the monopulse comparator circuit illustrated in Fig. 1. The second part of the test program was primarily concerned with the verification of the commutation network operating principle by the measurement of the complex output voltages of the waveguide commutator with the phase shifters in the circuit of Fig. 1 simulated by coaxial line stretchers and with a 6-dB directional coupler employed at the RF input. All measurements were made with a network analyzer with the swept frequency capability employed whenever possible.

The optimum output probe configuration of the commutator was readily arrived at and consisted of a design that employed tapered probes in contact with the coaxial waveguide inner conductor. The output tunable short circuit was positioned for optimum overall VSWR performance and this location was generally in the neighborhood of one-quarter of a free space midband wavelength from the probe plane. The input probe design was more of a problem and a number of modifications were required before a suitable probe design was obtained. The final input probe configuration chosen for the amplitude commutator measurements reported upon in this short paper employed tapered and noncontacting probes.

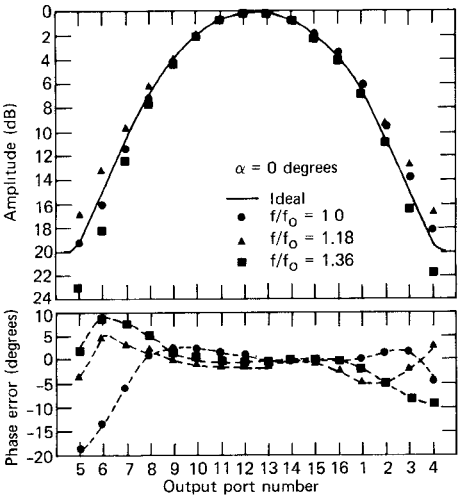

Fig. 3 Commutator output amplitude and phase measurements.

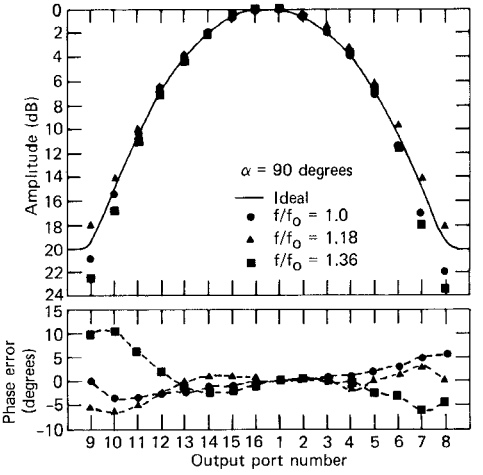

Fig. 4. Commutator output amplitude and phase measurements.

For the 30-percent bandwidth optimization, the measured TEM mode VSWR was less than 1.6 : 1 and for the TE_{11} modes, 1.8 : 1. The isolation between the input ports of the monopulse comparator, i.e., the TEM and TE_{11} mode generation ports, was better than 25 dB throughout the band. The insertion loss of the monopulse comparator circuit did not exceed 0.4 dB in the 30-percent frequency band, and the insertion loss of the coaxial amplitude commutator, while difficult to accurately measure, is in the 0.1-dB range.

Commutator Output Measurements and Antenna Pattern Performance

Figs. 3 and 4 present the coaxial waveguide commutator output port complex amplitude measurements made with a 6.0-dB input coupler and for the conditions of orthogonal TE_{11} mode excitation, i.e., $\alpha=0$, 90°, in the simulated variable power divider circuit of Fig 1. The measurements were made at three frequencies in the 30-percent frequency band as indicated with an ideal continuous cosine-squared-on-a-20-dB pedestal distribution shown for comparison. The degree of deviation of the measured voltage magnitudes from the ideal case is qualitatively indicative of the extent to which undesirable spurious mode generation primarily due to input probe amplitude and phase imbalance compositely affects the ideal commutator output voltages. There are, of course, other factors that perturb the output voltages but which are difficult to quantify. Among these are the different complex and multiple reflections in each channel, mechanical probe irregularities, and the errors inherent in the measurement process itself. It is also important to recognize the fact that the amplitude distribution measurements of Figs. 3 and 4 pertain to heavily tapered aperture excitations compatible with low-sidelobe idealized sum pattern performance. In the case of such large amplitude distribution tapers, the relatively small pedestal voltage tends to be more significantly perturbed by commutator unbalanced input probe excitation than would be a more modestly tapered amplitude distribution function.

A set of linear array patterns was generated using the measured data of Figs. 3 and 4 for complex amplitude element excitation. A linear array geometry was chosen because a perspective of array excitation error effect on the ideal low-sidelobe antenna pattern structure was being sought and the introduction of a finite radius of curvature was deemed an unnecessary complication. While the complex amplitude measurements of Figs. 3 and 4 may contain a background of random error, the more likely designation of the major error field would be one of systematic origin. Thus no attempt has been made to rms the error fields with the generated array patterns chosen as the more appropriate indicators of error effects.

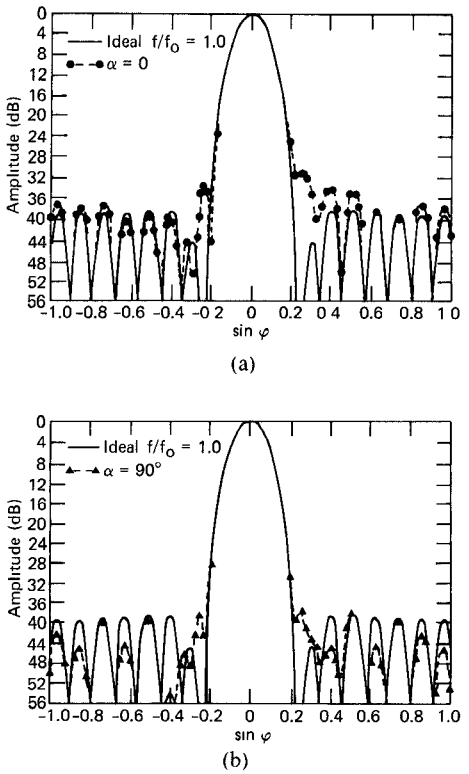

Fig. 5. Array antenna pattern performance for ideal and measured commutator output voltages.

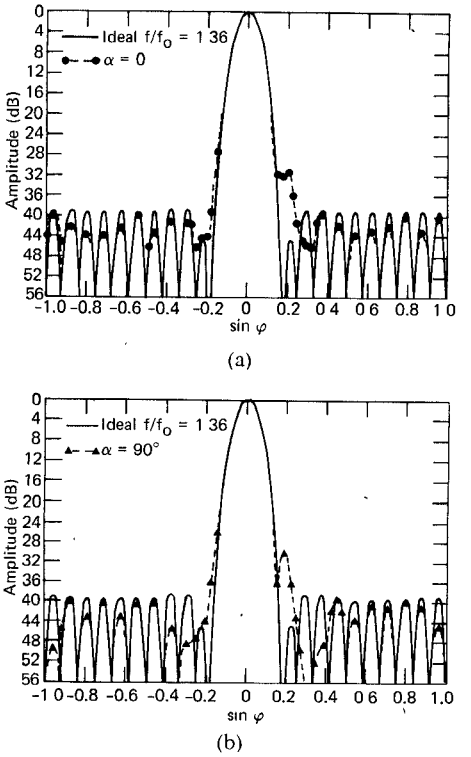

Fig. 6. Array antenna pattern performances for ideal and measured commutator output voltages.

Computed patterns for the low and high ends of the 30-percent frequency band are shown in Figs. 5 and 6 with the ideal patterns shown for comparison purposes. The array element spacing was 0.55 wavelength at the low-frequency end of the 30-percent band. An isotropic element pattern was assumed so that the off-axis sidelobe structure would not be muted with a directive element

gain pattern. While the sidelobe structure of the computed patterns deviates somewhat from the ideal errorless case, the results are nevertheless indicative of excellent low-sidelobe performance over a large frequency band.

Conclusions

A coaxial waveguide amplitude commutator has been developed that can be employed in the design of a low-sidelobe scanning circular array antenna. The resultant antenna efficiency of such a design will be relatively high because the RF feed commutator network insertion loss is small and on the order of 0.5 dB. This waveguide commutator feed design is suitable for circular phased arrays that are employed as communication or radar antennas.

Acknowledgment

The author wishes to thank numerous APL staff members who contributed to the success of this project.

References

[1] J. E. Boyns *et al.*, "A lens feed for a ring array," *IEEE Trans. Antennas Propagat.*, vol. AP-16, no. 2 pp. 264–267, Mar. 1968.
[2] B. Sheleg, "A matrix-fed circular array for continuous scanning," *Proc. IEEE*, vol. 56, pp. 2016–2027, Nov. 1968.
[3] R. S. Giannini, "An electronically scanned cylindrical array based on a switching and phasing technique," in *IEEE Int. Symp. Antennas Propagat. Dig.*, pp. 199–207, Dec. 1969.
[4] B. F. Bogner, "Circularly symmetric RF commutator for cylindrical phased arrays," *IEEE Trans. Antennas Propagat.* vol. AP-22, no. 1, pp. 78–81, Jan. 1974.
[5] N. Marcuvitz, *Waveguide Handbook* (MIT Radiation Laboratory Ser., vol. 10). New York: McGraw-Hill, 1951.
[6] A. R. Dion and L. J. Ricardi, "A variable coverage satellite antenna system," *Proc. IEEE*, vol. 59, no. 2, pp. 252–262, Feb. 1971.

Coupling Between Two Collinear Parallel-Plate Waveguides of Unequal Widths

YAKOUT E. ELMOAZZEN, MEMBER, IEEE, AND LOTFOLLAH SHAFAI, SENIOR MEMBER, IEEE

Abstract—**The problem of coupling between two collinear parallel-plate waveguides of unequal widths is investigated using the moment methods. The exciting mode of the waveguide is assumed as the incident field and an integral equation for the induced currents is expressed in terms of the reflected, the transmitted, and the evanescent currents on the walls of the waveguides. This integral equation is solved numerically and the results for the reflections and the transmission coefficients and the radiated field are obtained. The effect of varying the coupled waveguide width and the separation distance of the waveguides is investigated.**

I. Introduction

Both the Wiener–Hopf technique [1] and the moment method [2] were used by Elmoazzen to investigate the problem of coupling between two collinear parallel-plate waveguides of equal widths and separated by a certain distance. No attempt was made there to study the case of coupling between two waveguides of unequal widths. This work is devoted to the investigation of this problem. Since an exact solution is not known, a numerical method is used to solve the problem. It was shown in a previous paper [2] that an integral equation for the induced currents on the waveguides can be obtained in terms of the reflected, the transmitted, and the evanescent currents on the waveguides. The resulting integral equation was thus solved using the moment method [3] to find the desired currents. An application of the moment method to the problem reduces the integral equation to a set of linear simultaneous equations, the number of which depends on the number of propagating modes in the waveguides and the decay rate of the evanescent currents. Evanescent currents have significant values only near waveguide ends and need be considered only over a finite section of each waveguide end [4]. Once the reflection and the transmission coefficients as well as the evanescent currents are obtained, the radiation field can be obtained readily.

In the present work, a similar formulation is used to generate an integral equation for the currents on the waveguide walls. Pulse functions are utilized to describe evanescent currents and the integral equation is reduced to a set of simultaneous linear equations for the reflection and the transmission coefficients and the evanescent currents. The expressions for the elements of the coefficient matrix are obtained, which reduce to previous expressions [3] when waveguides have equal widths. The new expression for the radiation field is also given. Based on these expressions, a few numerical results are obtained and are presented in the last section.

II. Formulation of the Problem

A geometry of the problem is shown in Fig. 1. Assume a TE_{01} mode is propagating in the left waveguide, which has a width d. The coupled waveguide has a width $D=Fd$, where $F_{\min}<F<\infty$. To insure mode propagation in the coupled waveguide, it is assumed that $F_{\min}=\sin\theta_{01}=\lambda/2d$.

The incident, the reflected, and the transmitted currents on the walls of the exciting and the coupled waveguide are given by

$$J_z^i=\hat{z}\frac{1}{\eta}\sin\theta_{01}\exp(jkx\cos\theta_{01}) \tag{1}$$

$$J_z^r=\hat{z}\frac{R}{\eta}\sin\theta_{01}\exp(-jkx\cos\theta_{01}) \tag{2}$$

$$y=o,d, \qquad x>0$$

and

$$J_z^t=\hat{z}\frac{1}{\eta}\sum_{l=1}^{l_{\max}}T_l\sin\theta_{0l}\exp(jkx\cos\theta_{0l}) \tag{3}$$

$$y=-\frac{1}{2}(D-d),\frac{1}{2}(D+d), \qquad x<-L$$

where $l=1,3,5,\cdots$, $\eta=120\pi$, $\theta_{0l}=\sin^{-1}(\lambda l/2D)$, and $l_{\max}$ is determined by the fact that $\sin\theta_{0l_{\max}}$ must be smaller than unity. It is, therefore, given by $l_{\max}=$integer of $(2Fd/\lambda)$. In these equations, R and T_l are the reflection coefficient of TE_{01} mode and the transmission coefficient of TE_{0l} mode, respectively. The evanescent modes also contribute to the induced currents on the waveguides, but are significant only near waveguide ends. Representing these evanescent currents by $J_z^e=\hat{z}J_z^e$, the boundary con-

Manuscript received August 26, 1980; revised October 24, 1980.

Y. E. Elmoazzen is with the Electrical Department of Northern Alberta Institute of Technology, Edmonton, Alta., Canada

L. Shafai is with the Electrical Engineering Department, The University of Manitoba, Winnipeg, Man., Canada

0018-9480/81/0300-0270$00.75 ©1981 IEEE